

# How to Measure the Various Types of Geologic Porosities in Oil and Gas Reservoirs Using Image Logs

M. Alizadeh<sup>\*1,a</sup>, Z. Movahed<sup>1,b</sup>, R. Junin<sup>1,c</sup>, R. Mohsin<sup>1,d</sup>, M. Alizadeh<sup>2,e</sup> and M. Alizadeh<sup>3,f</sup>

<sup>1</sup>Faculty of Petroleum and Renewable Energy Engineering Universiti Teknologi Malaysia, 81310 (UTM) Johor Bahru, Johor, Malaysia

<sup>2</sup>Gachsaran Oil and Gas Production Company – GOGPC, 7581873849 Gachsaran, Iran

<sup>3</sup>Mechanical Engineering Department, Tarbiat Modares University, 14155-111 Tehran, Iran

<sup>a,\*</sup>mostafa.alizadeh88@yahoo.com, <sup>b</sup>zmovahed@gmail.com, <sup>c</sup>radzuan@petroleum.utm.my,

<sup>d</sup>rahmat@petroleum.utm.my, <sup>e</sup>alizadeh.me@gmail.com, <sup>f</sup>ymohsen.alizadeh@yahoo.com

**Abstract** – *Measuring the geologic porosity types including the primary porosity, secondary porosity, fracture porosity, vuggy porosity and so on is an important task in oil and gas reservoirs. Using the image log technology, this analysis can be done very well, but this process is complicated and still unknown to many researchers. Therefore, in this work using a unique case study and a number of valuable image log interpretation examples the process will be explained. Copyright © 2015 Penerbit Akademia Baru - All rights reserved.*

**Keywords:** Geologic porositie, Oil and gas reservoirs, Image logs

## 1.0 INTRODUCTION

Gachsaran oil field is in the southwest of Iran (Figure 1) with an anticline structure, made of anhydrite/salt, 80 km long, 300 m-1500 m thickness, 8-18 km wide; it provides an excellent seal for the Asmari reservoir, the Pabdeh reservoir, the Gurpi reservoir and the other reservoirs (Figure 2) [1].

Most carbonate formation evaluation methods rely on traditional resistivity and porosity logs. For many carbonate reservoirs, the correlation between hydrocarbon production and density-neutron logs has been inconsistent. Good production has been obtained from intervals where logs show low porosity whereas zones having higher porosity have not produced. Total production from carbonate reservoirs in mature fields has often been greater than expected from standard porosity logs [4].

Many productive carbonates have complex dual porosity systems with widely varying proportions of primary and secondary porosity. The secondary porosity may contain vugs, moulds (oomoulds or biomoulds), channels, and fractures. Moreover, the originally homogeneous matrix / intergranular primary porosity may become patchy through selective cementation of the matrix. On the conventional porosity logs (density, neutron, and sonic), these porosity types often appear somewhat uniformly distributed. Moreover, due to coarse resolution of the conventional tools, such types of porosity get under-estimated or

overlooked. Borehole electrical images, FMI (Formation Micro Imager) in particular, provide both high resolution and azimuthal borehole coverage to resolve quantitatively the heterogeneous nature of porosity components [5].

In this work, 2 wells located in Gachsaran oil field will be selected, and the porosity analysis will be done in these wells by using the image logs and the other geological logs interpretation. The porosity analysis will be done in order to both having a better understanding of porosity system in this field and also explaining the methodology by showing the selected log interpretation examples.

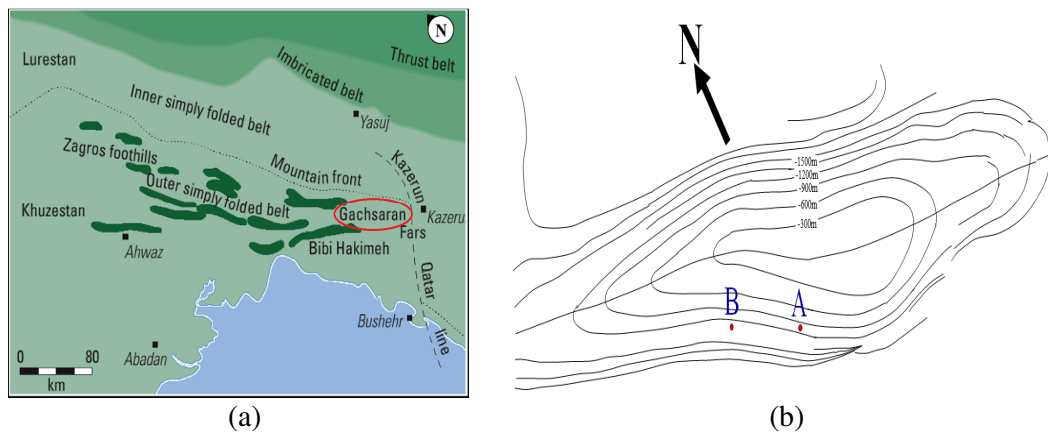


**Figure 1:** a) Location of the Gachsaran field [2]; b) UGC map of the Gachsaran field and the studied wells (GS-A and GS-B)

## 2.0 MATERIALS and METHODS

Borehole imaging delivers micro resistivity and acoustic images of the formation in both water-based and nonconductive mud. Borehole imaging is the preferred approach for determining net pay in the laminated sediments of fluvial and turbidite depositional environments. The FMI has a four-arm eight-pad array (i.e., four pads and four flaps as shown in Figure 3). Each pad and flap contains 24 buttons to make 192 buttons total for all four pads and four flaps. The tool includes a general purpose inclinometer cartridge, which provides accelerometer and magnetometer data. The tri-axial accelerometer gives speed determination and allows re-computation of the exact position of the tool. The magnetometers determine tool orientation. During logging, each microelectrode emits a passive, focused current into the formation. The current intensity measurements, which reflect micro resistivity variations, are converted to variable-intensity gray or color images. The observation and analysis of the images provide information related to changes in rock composition, texture, structure or fluid content (Figure 3) [6].

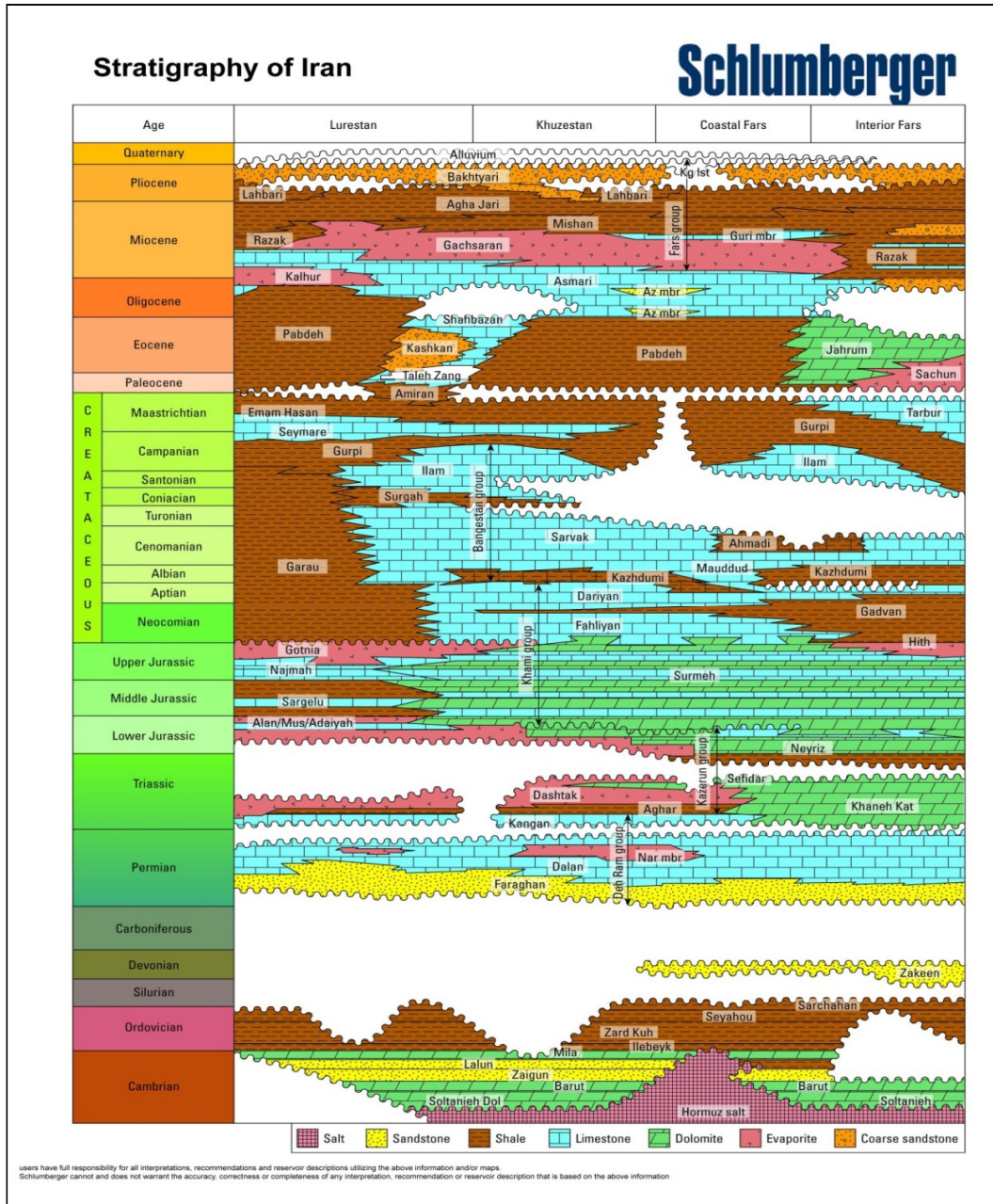


**Figure 2:** Picture showing the Gachsaran field overlying the Asmari, Pabdeh, Gurpi and other reservoirs, and stratigraphic nomenclature of rock units and age relationships in the Zagros basin [3]

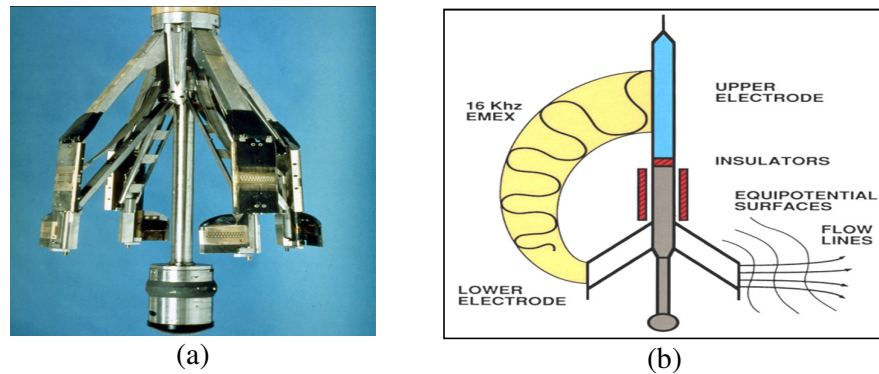


**Figure 3:** (a) Picture of FMI tool (b) explanation of the principle of measurement. EMEX current flows into the formation from the FBCC (upper electrodes) housing to pad section (which is the FMI sonde section carrying 192 imaging micro-electrodes), called lower electrode. Tool scale for Length is 7.75 m and for outside diameter is 12.70 cm

Schlumberger company has introduced a new approach to utilize borehole electrical images in the analysis of carbonate reservoirs porosity system. Through this technique porosity distribution and quantity of vugs / moulds fraction can be obtained. However, the results of the technique are affected largely by shale and bad hole conditions. In case the quality of one or two images is largely affected due to damaged FMI pad / flap or bad hole, such images can be discarded during the analysis.

The primary assumption for this technique is that the resistivity data from the electrical images is measured in the flushed zone of the borehole. The electrical images are then transformed into a porosity map of the borehole after their calibration with the shallow resistivity and log porosity (preferably effective porosity). Following equation is used to get such transformation; it takes log porosity (effective log porosity being the best option), any shallow resistivity measurement (mostly LLS or SFLU), and conductivity of individual FMI electrodes / buttons ( $C_i$ ) as inputs.

$$(\varphi)_{fmi} = (\varphi)_{log} * [LLS * C_i]^{1/m} \quad (1)$$

where  $C_i$  is conductivity of each FMI electrodes,  $m$  is cementation factor, and  $\varphi_{log}$  is log porosity.

For this work, synthetic average FMI resistivity (SRES) will be used as resistivity and PXND (porosity derived from cross plot density-neutron logs) as log porosity to be input into the above equation. Ideally effective log porosity should be used which is derived from the log analysis. Since no log analysis was carried out, therefore simple cross-plot neutron-density porosity will be used for this study. The cementation factor ( $m$ ) will be 1.9 for the whole interval of each formation. Automated analysis of this porosity map, windowed over short intervals (generally 1.2 inch), provides a continuous output of primary and macro-secondary porosity components of rocks. At every specified sampling rate (generally 0.1 inch for oomouldic porosity system or 0.3 inch or bigger for formations having large size vugs or moulds), porosity distribution histograms will be computed. The homogeneous carbonate intervals give narrow unimodal distribution (Figures 4 and 5).

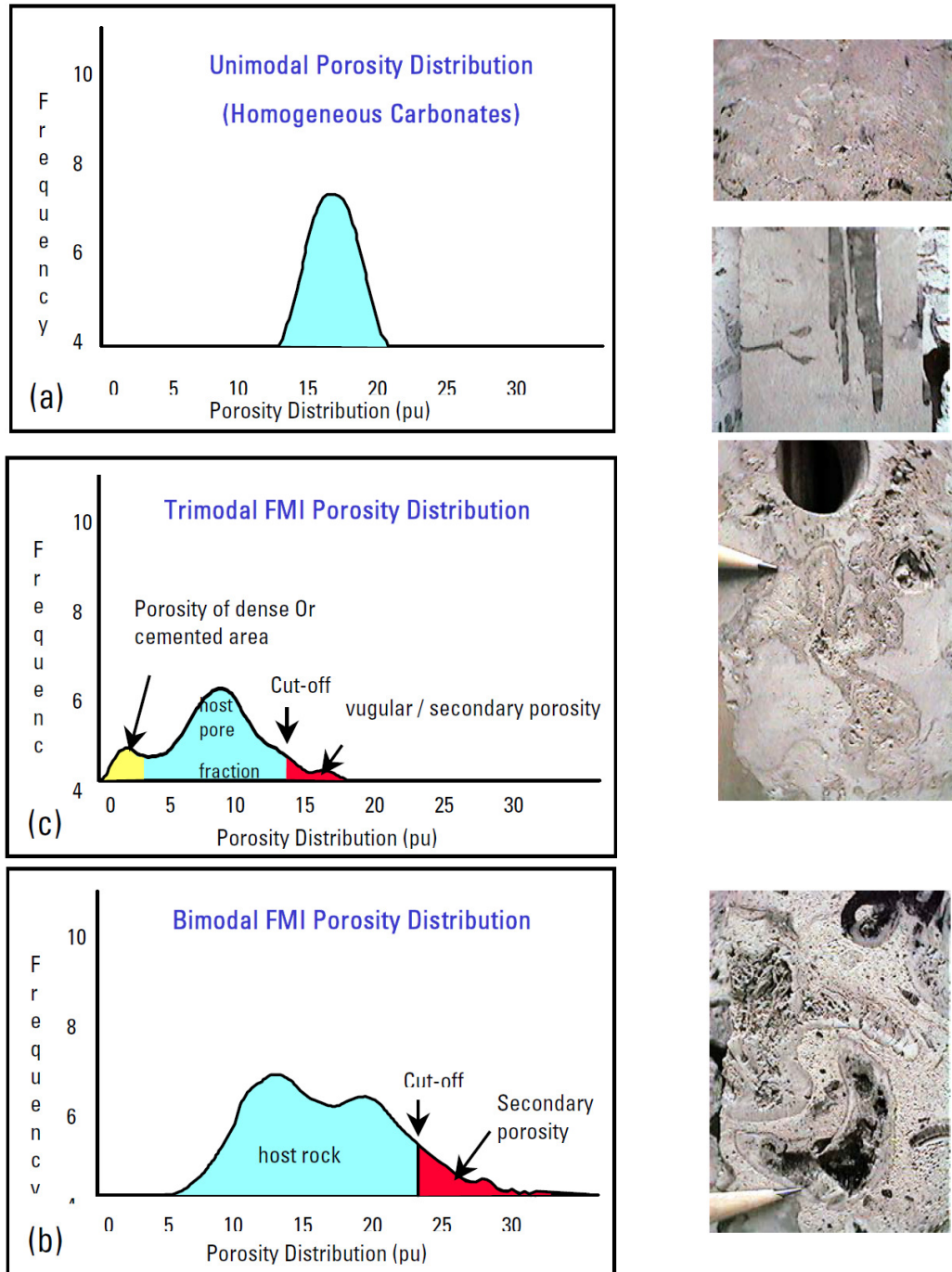


**Figure 4:** Explanation of the method used for porosity analysis from FMI and logs. Typical FMI porosity histograms showing porosity distributions in homogeneous and heterogeneous carbonates. Unimodal distribution is found in homogeneous carbonates (a). While bimodal to trimodal distributions are found in heterogeneous carbonates (b and c). The porosity component due to vugs and fractures is obtained by applying an empirical cut-off to the porosity histograms (scale for pictures is given by showing a pencil)

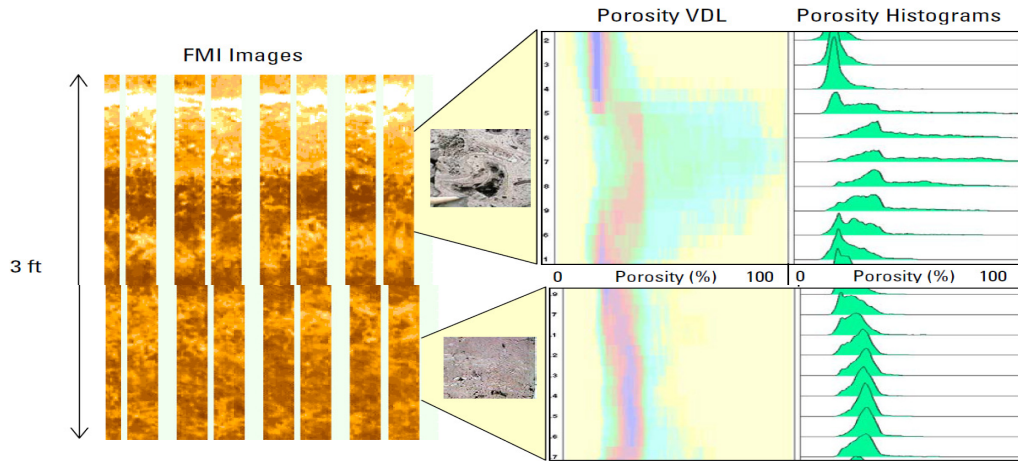


**Figure 5:** Example of porosity analysis from FMI and Logs showing difference in vuggy and non-vuggy sections of a rock

In vuggy carbonates, highly skewed unimodal or bimodal distribution of porosity is observed. While in the most heterogeneous carbonates where cementation, primary porosity and vuggy porosity are present, highly skewed and broad or bimodal / trimodal porosity distribution may be observed. On such histograms, the points from the high porosity ends represent leached pores (vugs or moulds) and fracture fractions of porosity. Whereas the points from the low porosity end belong to the dense or cemented areas of the host rock (Figure 6).

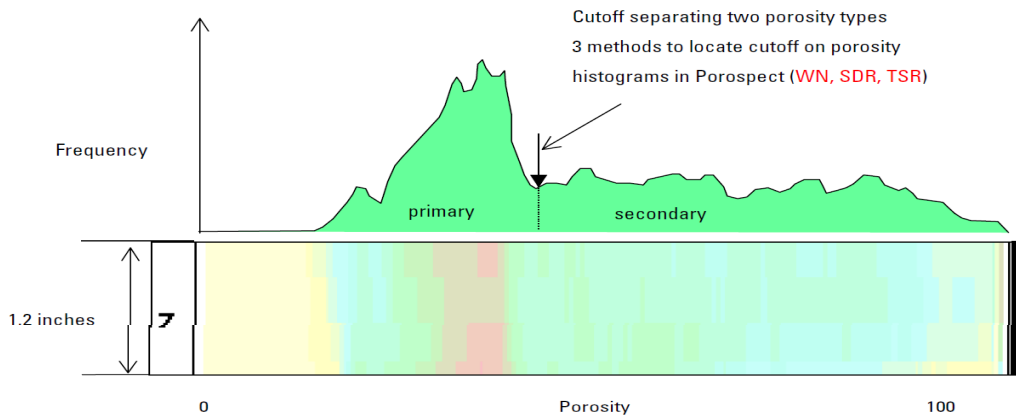


**Figure 6:** Figure explaining porosity VDL (variable-density-log) generation from Porosity histograms

The area under the high porosity tails of porosity histograms gives quantity of secondary porosity. A continuous / moving threshold or cutoff is applied to the porosity histograms to separate the contribution of secondary pores from the host pore fraction, which may be comprised of primary interparticle / intraparticle pores and secondary micro-pores (that are not seen by the FMI). So the porosity points above the threshold correspond to the macro-secondary pores and the one below correspond to host pores. There are three different types

of thresholds / cutoffs that are applied to the porosity data. The description of each method is given below:

**WN Threshold Method:** In this method, first the standard deviation of the histogram below the median porosity is computed. Then the cutoff / threshold is obtained by adding a multiple of this standard deviation to the median porosity. Generally the value of the multiple is taken as 3; however this is not fixed. It can be increased or decreased based on the calibration of the porosity results with cores.

**SDR or Fixed-Percentage Threshold Method:** This is a variant of WN method. It locates the threshold at a fixed percentage (typically 15 %) above the mean porosity. The percentage value is not fixed. It may be greater or smaller than 15 %. Core observation / measurement provides a way to fix its value.

**TSR or Discriminant Threshold:** This method does not require any user input to define the threshold. It involves the use of *Discriminant Threshold Selection Algorithm*, which is based on the standard linear discriminant analysis used in the field of pattern recognition and statistics. This method works on the idea that if the porosity data consists of two populations, then the best threshold should maximally separate the two means.

Average of the overall porosity seen collectively by all (192) FMI buttons / electrodes is also computed. Across the homogeneous carbonate intervals, which compute unimodal porosity distribution, the average of the image porosity reads nearly the same as the effective log porosity. The unimodal porosity distribution changes into bimodal or trimodal or broad distribution across the heterogeneous carbonate intervals. The average image porosity across such intervals may be either more or less than the effective log porosity depending upon the type of heterogeneity, i.e., dense areas, vugs, moulds, fractures, matrix patches of very high porosity, dense streaks or high porosity streaks.

### 3.0 RESULTS AND DISCUSSION

#### 3.1 Porosity Analysis for the Well Number GS-A

##### 3.1.1 Porosity System

The accuracy of porosity analysis from the image logs is largely dependent on the selection of right values for the parameters used in the analysis. Therefore some priori knowledge about the type and size of secondary pores is required for the rocks to be evaluated with the imaging tools. Since no core data was available for that purpose in the study well, therefore analysis was carried out in such a way that whole range of macro-secondary pores could be addressed. The porosity analysis was carried out to provide macro-secondary porosity (vugs / moulds) and high-resolution porosity for Asmari formation. The porosity results (secondary porosity and high resolution porosity) are output at 0.1 inch and 1.5 inch. While the porosity histogram / VDL display is output at 1.5 inch. All porosity results (secondary porosity, porosity minimum and maximum limits, and high resolution porosity) from the study well are displayed at 1.5 inch in the (Figures 7 & 8). The results of porosity analysis are discussed in the following.



### 3.1.2 Vuggy / Mouldic Porosity

As indicated by the higher porosity tails of porosity histograms / VDL, there are some sections in Asmari which appear to be vuggy / mouldic. The vuggy / mouldic porosity (also called secondary porosity in the report to include all components of leached pores) was then computed by applying an optimal dynamic cutoff to the porosity histograms to compute the area under the high porosity tails. A multiplier of 3.0 was used for the WN method and 15% for the SDR method.

Previous studies on carbonates, using FMI, logs and cores, indicated that TSR method generally gives better results for secondary porosity computation from porosity VDL / histograms. So it is assumed that secondary porosity estimated by TSR method in the study well is possibly better than the other two threshold methods. However, cores would be needed to determine which cutoff method gives optimum results for secondary porosity computation in the Asmari formation. The secondary porosity outputs by WN and TSR methods are displayed in the composite plot to represent possible minimum and maximum limits of secondary porosity, respectively.

The secondary porosity (possibly due to dissolution) varies from 0 to 10% with some intervals showing higher secondary porosity than 10%. Such zones are not possibly showing realistic secondary porosity because it is affected by the input log porosity, which is raw cross-plot density-neutron porosity.

The zones with broader porosity distribution are the one that computed higher secondary porosity. Such zones include: 1867-1874m, 1943-1947m, 1951-1953m, 1962-1965m, 1970.5-1973.5m, 1986.5-1988m, 1998-2001m, 2008-2022, 2038-2040m, 2043-2061m, 2067-2071m, 2075-2079m, 2090-2095m, 2116-2121m, 2137-2143m, 2150-2152m, 2162-2164m, 2170-2173m, 2214-2218m, 2255-2256.5m, 2303-2306m, 2313-2316m, 2326-2329m, 2424-2435m and 2437-2443m (Figures 9 and 10).

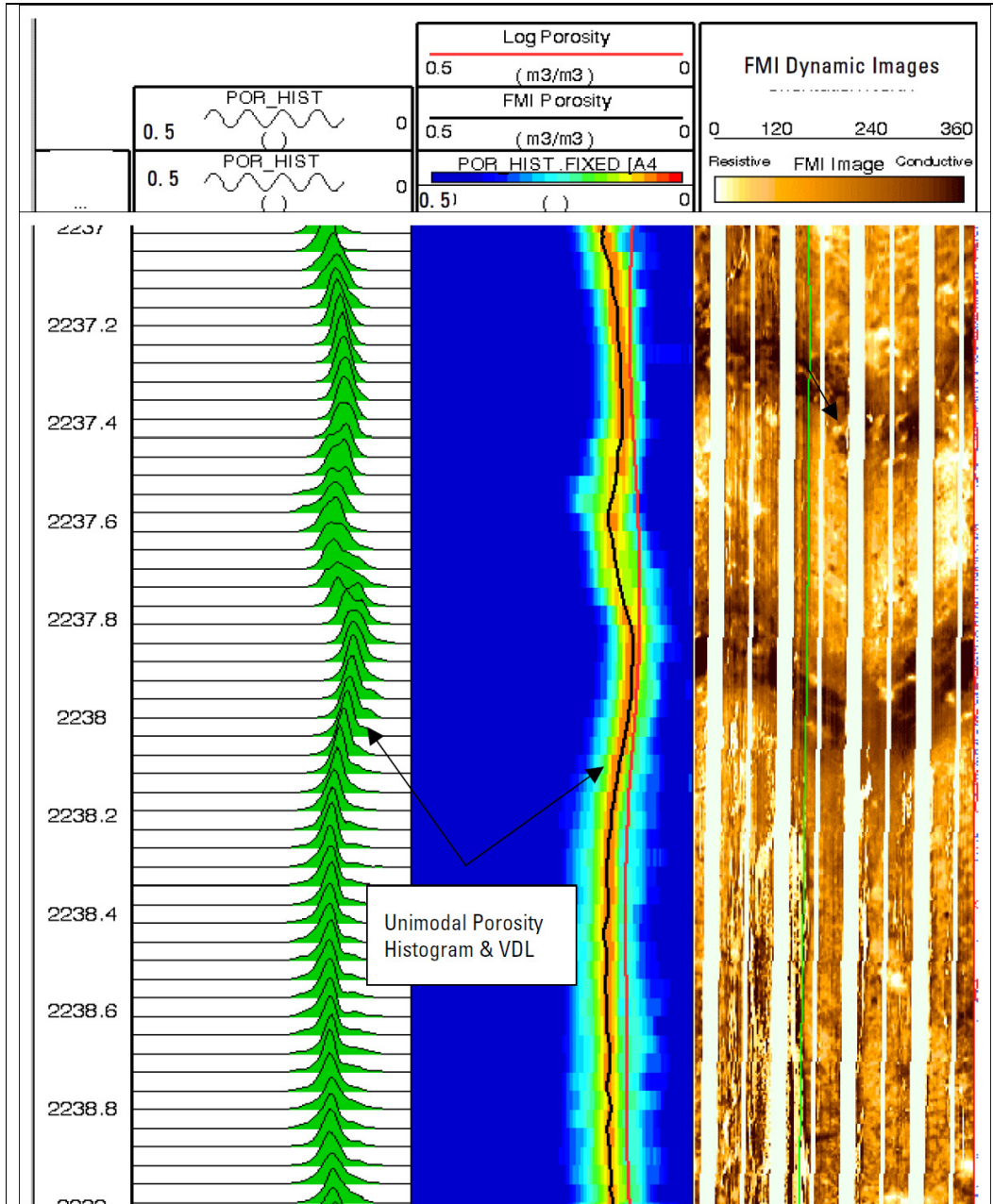


**Figure 9:** Narrow range of porosity shown by porosity-VDL (variable-density-log) and porosity-histograms in a section of Asmari indicates its homogeneous nature

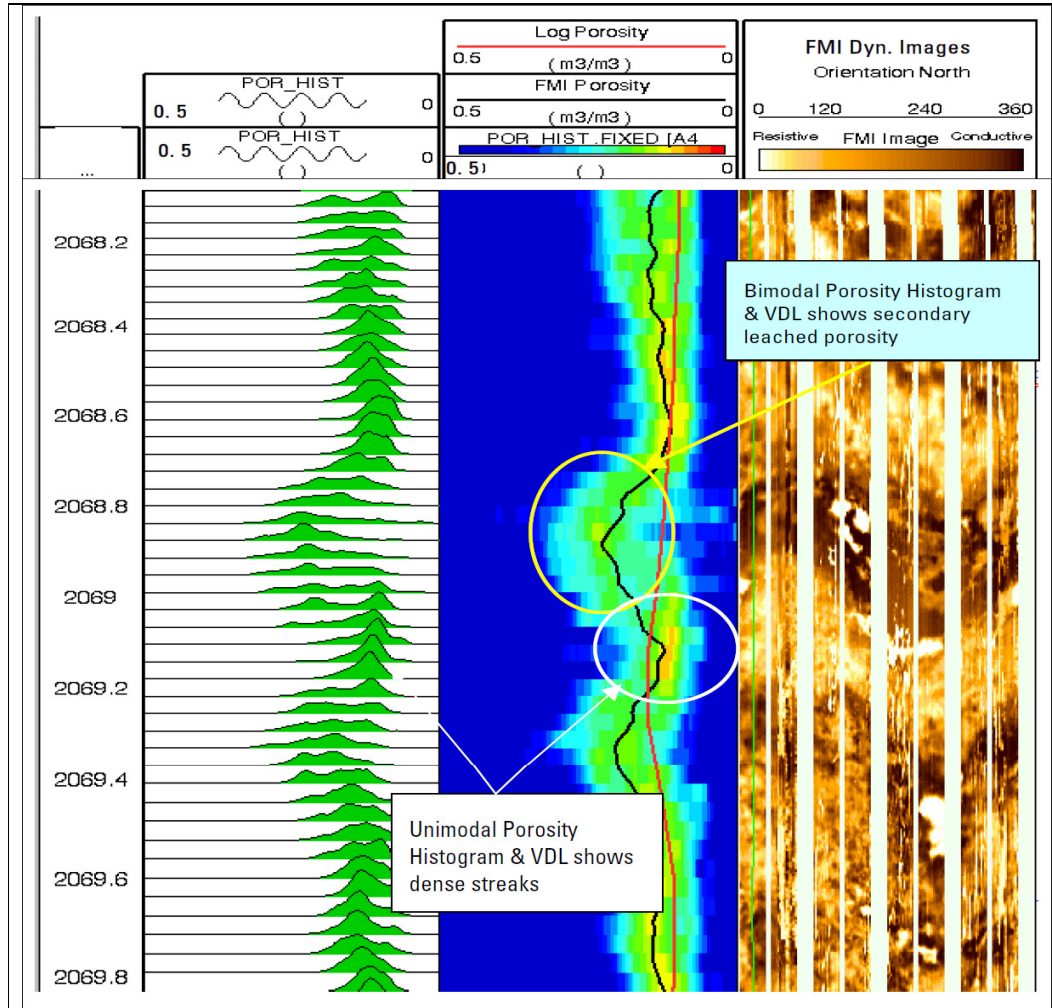


**Figure 10:** Porosity VDL (variable-density-log) and histogram display over a section of Asmari Formation showing presence of secondary / leached porosity as indicated by high porosity tails on FMI transformed porosity histograms and VDL displays

### 3.1.3 High-Resolution Porosity Array and Porosity VDL

It is obtained from the average of the porosity map / histograms constructed from 192 porosity channels around the well bore. For the current well, it was output at 0.1 inch depth sampling. Based on their comparison with the effective log porosity and core porosity, following observations have been made:

- High and low porosity layers / streaks of smaller thickness, not resolved by the conventional porosity logs, get highlighted on the high-resolution porosity. The high resolution FMI porosity tends to match with the cross-plot density-neutron porosity over the homogenous zones while it reads less than the log porosity over the heterogeneous intervals having broader porosity distribution.
- Porosity histograms and VDL display indicates that more than half interval of Asmari formation is heterogeneous in terms of porosity distribution as indicated by wide porosity distribution. However, there are some zones which have narrow and dominantly unimodal

distribution of porosity. Such zones include 1847-1867m, 1890-1941m, 2022-2037m, 2129-2136m, 2147-2162m, 2203-2209m, 2222-2226m, 2232-2236m, 2242-2259m, and 2316-2390m.

The importance to know the occurrence of high porosity streaks (which may also have high permeability) increases more when the field enters injection phase because such layers / streaks may cause early break-through of injected water / gas from the injectors. Similarly the thin dense streaks / layers, which may go undetected with the conventional logging techniques, may act as barriers or baffles for the vertical flow of the reservoir fluids.

### 3.2 Porosity Analysis for the Well Number GS-B

#### 3.2.1 Porosity System

The accuracy of porosity analysis from the image logs is largely dependent on the selection of right values for the parameters used in the analysis. Therefore some priori knowledge about the type and size of secondary pores is required for the rocks to be evaluated with the imaging tools. Since no core data was available for that purpose in the study well, therefore analysis was carried out in such a way that whole range of macro-secondary pores could be addressed. The porosity analysis was carried out to provide macro-secondary porosity (vugs / moulds) and high-resolution porosity for Asmari and Pabdeh formations.

The porosity results (secondary porosity and high resolution porosity) are output at 0.1 inch and 1.5 inch. While the porosity histogram / VDL display is output at 1.5 inch. All porosity results (secondary porosity, porosity minimum and maximum limits, and high resolution porosity) from the study well are displayed at 1.5 inch in the (Figures 11 and 12). The results of porosity analysis are discussed in the following.

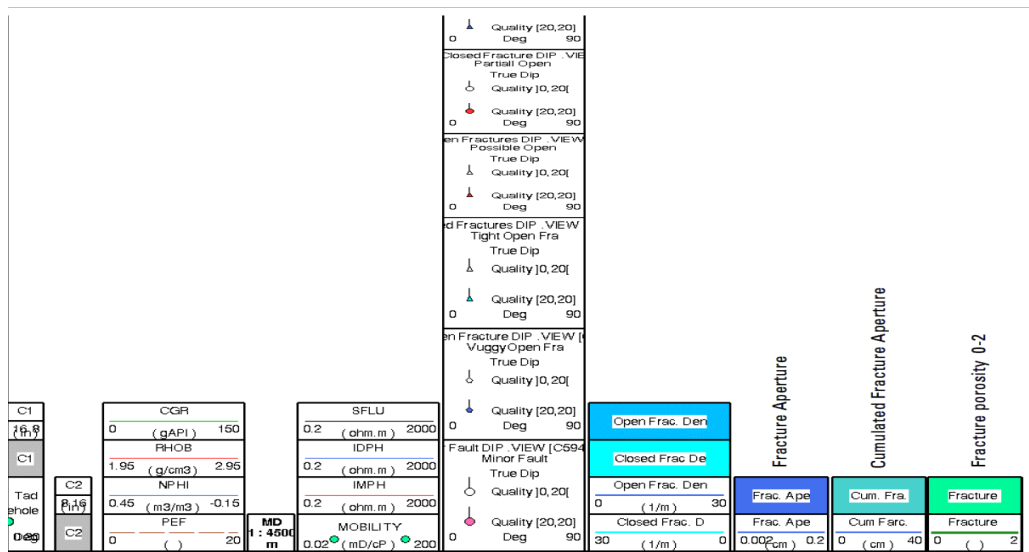
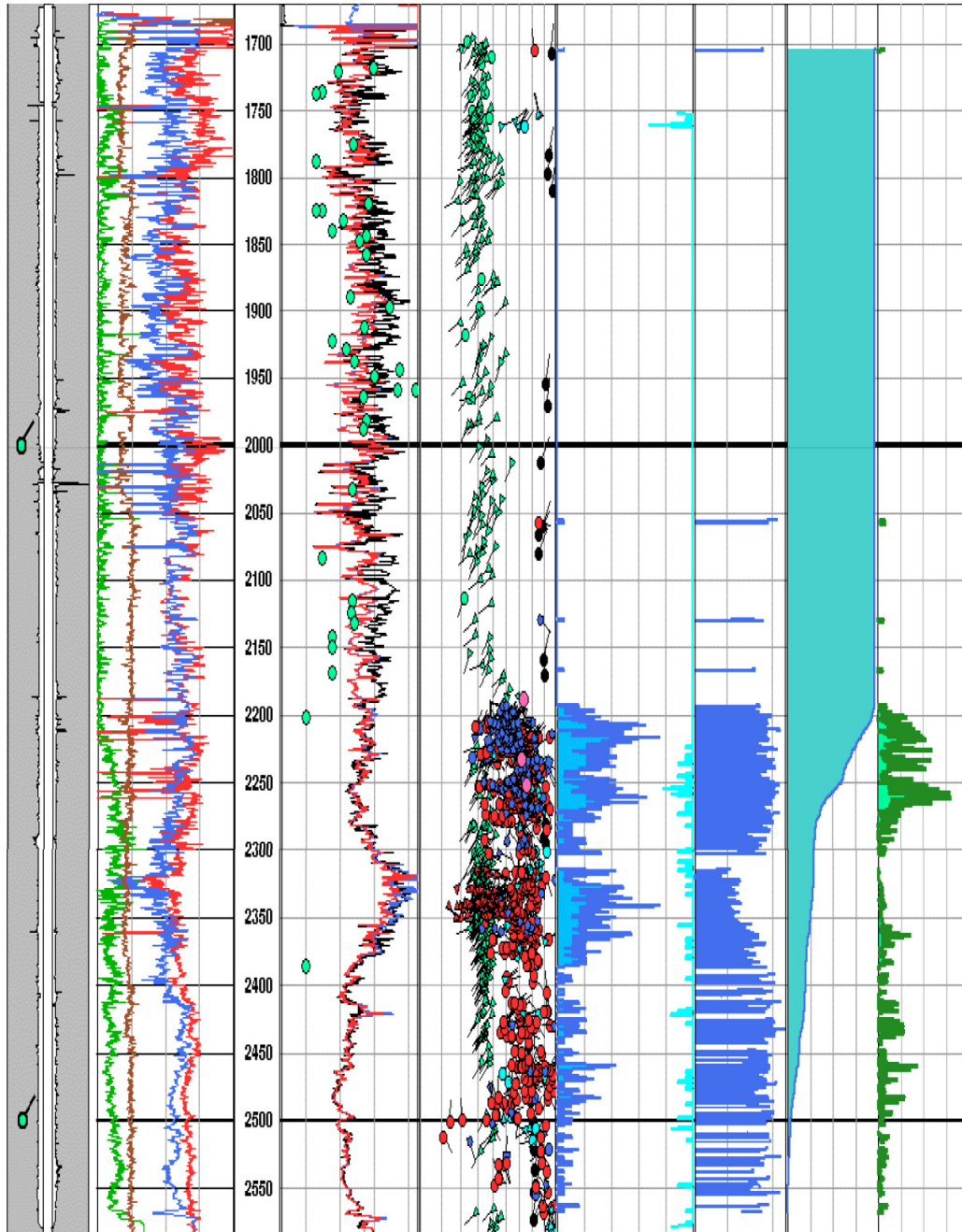


Figure 11: Header for the summary plot of figure 12



**Figure 12:** Summary log of resistivity, density, porosity, dips, fractures density and apertures in Asmari, Pabdeh and Gurpi formations

### 3.2.2 Vuggy / Mouldic Porosity

The secondary porosity (possibly due to dissolution) varies from 1 to 20% with some intervals showing higher secondary porosity than 20%. The secondary porosity in the study well is largely affected by the image quality; hence cannot be used as such for quantitative purposes. The image quality is affected mainly by the badhole in some places, by the change of oil-base mud to oil-water emulsions, and by the presence of shale / clays particularly in

Pabdeh and Gurpi. So the secondary porosity in this case can be used only in qualitative sense for comparing one zone with the other.

The intervals with broader porosity distribution are the heterogeneous ones and they computed higher secondary porosity. Intervals having various range of secondary porosity are given in the following table to highlight the zones of higher possible productivity associated with higher amount of secondary / dissolution pores (Table 1).

**Table 1:** Porosity distribution

Porosity Distribution		Secondary Porosity Intervals			Figures
Broad	Narrow	Porosity Range 2 – 5 %	Porosity Range 5 – 8 %	Porosity Range 8 % - Above	
1714-1722	1736-1820	1740-1820	1718-1725	1747-1749	Enclosure-1
1732-1736	1874-1886	1965-1980	1732-1738	1813-1815	
1820-1834	1928-1936	1996-2044	1820-1854	1819-1821	
1836-1874		2052-2082	2045-2053	1895-1903	
1886-1928		2154-2164	2080-215-	1927-1930	
1936-1964		2190-2198	2174-2182	1955-1960	
1986-1994		2220-2240	2198-2115	2186-2199	
2044-2052		2256-2348	2348-2363	2211-2213	
2084-2186		2380-2570			

### 3.2.3 High-Resolution Porosity Array and Porosity VDL

It is obtained from the average of the porosity map / histograms constructed from 192 porosity channels around the well bore. For the current well, it was output at 0.1 inch depth sampling. Based on their comparison with the effective log porosity and core porosity, following observations have been made (Figures 13 and 14):

- High and low porosity layers / streaks of smaller thickness, not resolved by the conventional porosity logs, get highlighted on the high-resolution porosity. The high resolution FMI porosity tends to match with the cross-plot density-neutron porosity over the homogenous zones while it reads less than the log porosity over the heterogeneous intervals having broader porosity distribution.
- Porosity histograms and VDL display indicates that more than half interval of Asmari formation is heterogeneous in terms of porosity distribution as indicated by wide porosity distribution. However, there are some zones, which have narrow, and dominantly unimodal distribution of porosity. Such zones include: 1706-1818m, 1924-1932m, 1961-1986m, 1994-2035m, 2052-2084m, and 2186-2240m. The VDL image shows, Pabdeh and Gurpi Formations are homogeneous in terms of porosity distribution.

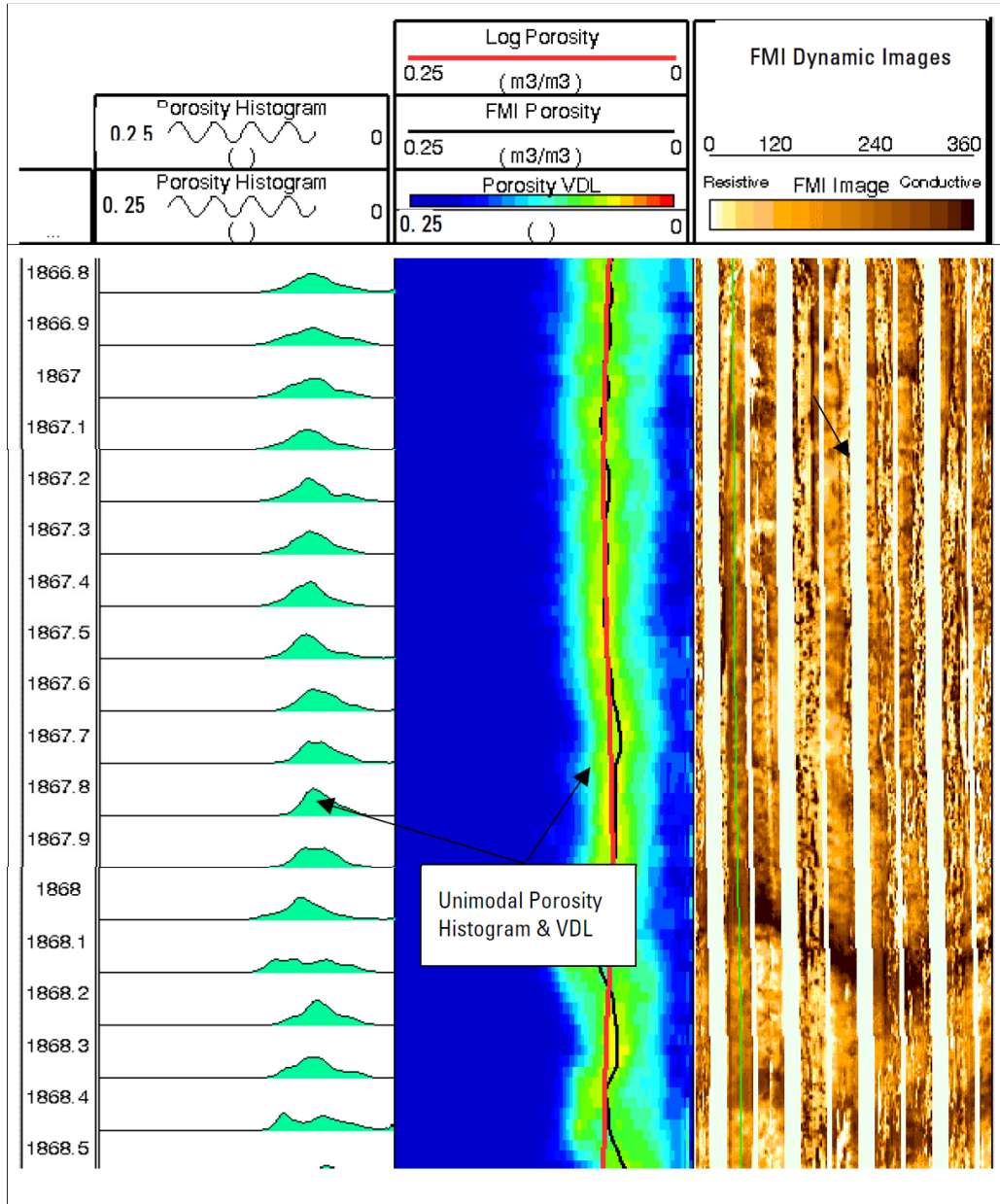


**Figure 13:** Narrow range of porosity shown by porosity-VDL (variable-density-log) and porosity-histograms in a section of Asmari indicates its homogeneous nature

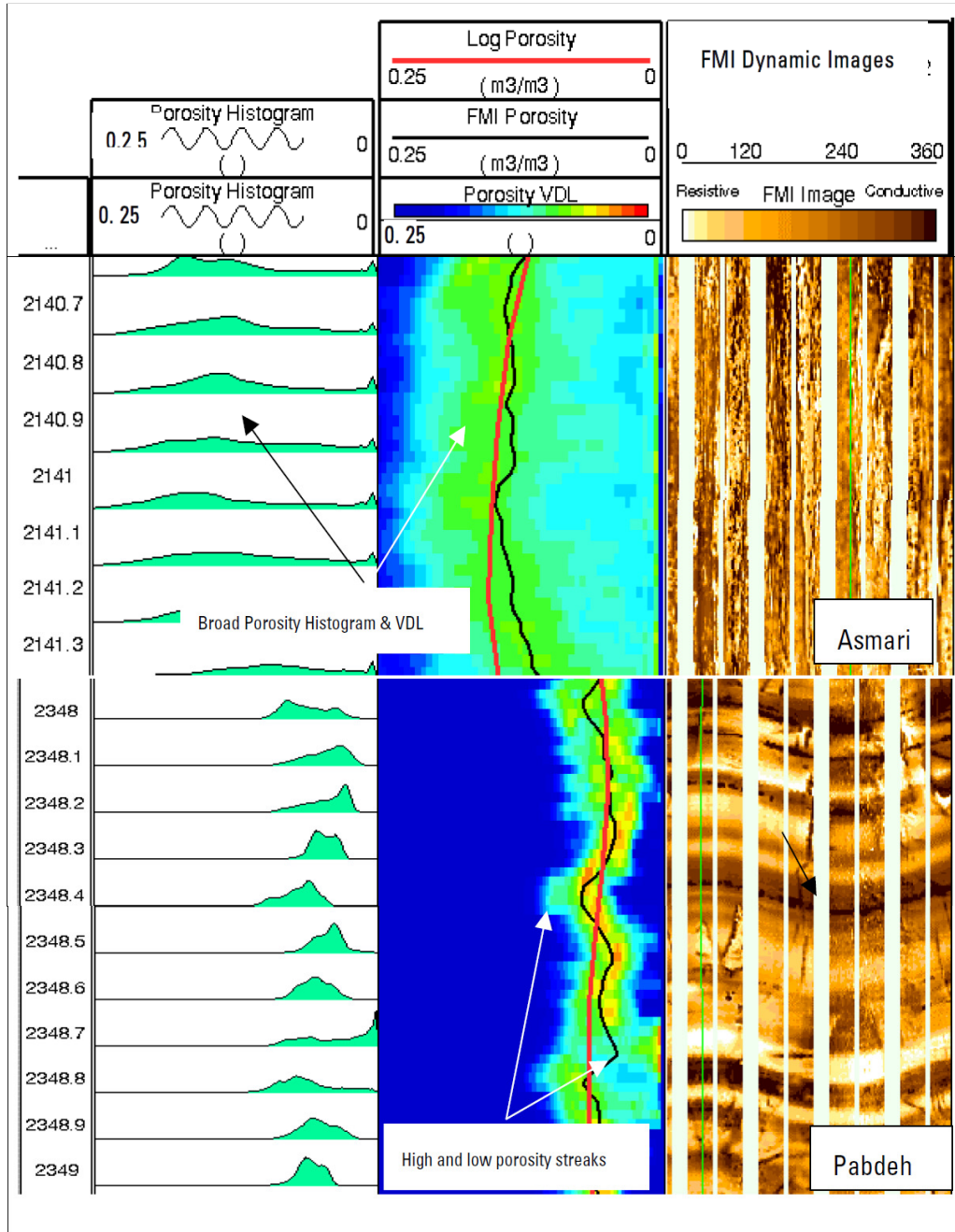


**Figure 14:** Porosity VDL (variable-density-log) and histogram display over sections of Asmari and Pabdeh formations. The section from Asmari formation is showing broad distribution, which is a result of bad quality image affected by bad borehole conditions. High and low porosity streaks are indicated by porosity VDL and average porosity curve (black)

#### 4.0 CONCLUSION

This work shows that how image log technology can be used to do the porosity analysis in oil and gas reservoirs. It is an example of porosity analysis that was done in Gachsaran field,

located in south of Iran. In this paper, the method in which the detailed information about the porosity system can be calculated in oil and gas reservoirs is explained.

## REFERENCES

- [1] F. Khoshbakht, H. Memarian, M. Mohammadnia, Comparison of Asmari, Pabdeh and Gurpi formation's fractures, derived from image log, *Journal of Petroleum Science and Engineering* 67 (2009) 65-74.
- [2] Z. Movahed, R. Junin, Z. Safarkhanlou, M. Akbar, Formation evaluation in Dezful embayment of Iran using oil-based-mud imaging techniques, *Journal of Petroleum Science and Engineering* 121 (2014) 23-37.
- [3] M. Alizadeh, Z. Movahed, R. Junin, W.R. Wan Sulaiman and M.Z. Jaafare, Fault Interpretation Using Image Logs, *Applied Mechanics and Materials* 695 (2014) 840-843.
- [4] Z. Movahed, Enhanced reservoir description in carbonate and clastic reservoirs, Paper presented at the SPE Asia Pacific oil & Gas Conference and Exhibition, Jakarta, Indonesia, 30 October-1 November (2007).
- [5] F. Khoshbakht, M. Azizzadeh, H. Memarian, G.H. Nourozi, S.A. Moallemi, Comparison of electrical image log with core in a fractured carbonate reservoir, *Journal of Petroleum Science and Engineering* 86 (2012) 289-296.
- [6] M. Alizadeh, Z. Movahed, R. Junin, W.R. Wan Sulaiman and M.Z. Jaafare, Image Logs Application for Locating Faults in Oil and Gas Reservoirs, *Advanced Research in Applied Mechanics* 3 (2015) 1-8.